8 May 1964

RSIC-179

TORSION OF ROUND SHAFTS WITH VARIABLE DIAMETER

By

Rudolf Sonntag

Translated from
Zeitschrift für Angewandte Mathematik und Mechanik,
9, No. 1, 1 - 22 (1929)

NOTICES

DDC Availability: Releasable without limitations on dissemination other than imposed by security classification.

Publicly Available from: Office of Technical Services, Department of Commerce, Washington 25, D. C.

Disclaimer. The findings in this report are not to be construed as an official Department of the Army position unless so designated by other authorized documents.

Disposition. Destroy this report when it is no longer needed. Do not return it to the originator.

8 May 1964 RSIC-179

TORSION OF ROUND SHAFTS WITH VARIABLE DIAMETER

By

Rudolf Sonntag

Translated from
Zeitschrift für Angewandte Mathematik und Mechanik,
9, No. 1, 1 - 22 (1929)

Translated from the German by
U. S. Joint Publications Research Service

Translation Branch
Redstone Scientific Information Center
Directorate of Research and Development
U. S. Army Missile Command
Redstone Arsenal, Alabama

JB

TORSION OF ROUND SHAFTS WITH VARIABLE DIAMETER[1)]
(A Contribution to the Theory of Notch Effects)

by Rudolf Sonntag, Gera

Zeitschrift für angewandte Mathematik und Mechanik [Journal of Applied Mathematics and Mechanics], February 1929, Vol 9, No 1, pp 1-22.

It is very important for the technology of machines to know about the stress increase which takes place, e.g., in shouldered-off shafts through the influence of diametric changes with relatively small fillet radii. This importance, however, is frequently underrated in practice, as is manifested by the all too often occurring and sometimes disastrous shaft breakdowns which can almost always be attributed to insufficient consideration of the stress increase during design and manufacture of such shafts. This adverse effect endangers particularly those shafts which are subjected during operation to rapidly changing torsional moments (e.g., torsional vibrations), since a slight excess over the elastic limit is all that is needed at each inversion to cause a rupture in course of time.

Corresponding to the importance of this matter, attempts were not lacking to find solutions for this, by no means simple, strength problem[2)], since A. Föppl [3)] laid its foundations by

1) Excerpt from author's doctoral thesis of the same title, accepted by the Polytechnic Institute of Munich, 1926. (Reviewers: Prof. Dr. phil. L. Föppl, Prof. Dr.-Ing. D. Thoma).

2) See the summarizing report by Th. Pöschl: Solutions of the Torsional Problem of Bodies of Rotation, published hitherto. This journal, Vol 2 (1922), pp 137-147.

3) A. Föppl: Report of the Meeting of the Bavarian Academy of Sciences 1905, Vol 35, p 249 and following, and A. and L. Föppl: Drang und Zwang [Strain and Stress], Vol 2, Second Edition, p 102 and following.

formulating the differential equation. However, only very little has been achieved as yet analytically because the rigorous integration of the differential equation at prescribed limiting conditions meets with severe difficulties, that have been overcome so far for only two extreme cases, which, however, are never encountered in practice (shaft with completely surrounding semicircular groove of infinitesimally small fillet radius[1] and a shaft with sharp shoulders[2] and abrupt changes in diameter). There are no numerical approximated solutions for the case of finite transition radii with the exception of a rough estimate made by A. Föppl[3], according to which the maximum strain in the fillet of a stepped shaft, the radius of which is 1/10 of the smaller shaft radius, is 2.09 times greater than the circumferential strain of the thinner part of the shaft.

The understanding of the stress distribution was appreciably advanced by a graphical integration method devised by Runge, by means of which F. A. Willers investigated, in his Göttingen dissertation[4], a great number of shaft forms of practical importance with respect to their maximum stresses, and did this with such exactness that his results can be considered as almost equivalent to actual stress measurements on a real shaft, provided that the material is isotropic. Unfortunately, the usefulness of this method is very limited in technical practice since it is excessively cumbersome and time-consuming, and also because the results found so far can only be given in graphical or table form.

The aim of the present paper is to provide the designer with reliable formulae for the calculation of the stress increases on the places of transition in coaxial shafts used in machine design; these formulae shall at the same time be simple enough to establish their place in practice and in the technical handbooks.

The solutions given are approximations. For testing their accuracy we had available the values found by Willers as well as the results of our own laboratory tests. The following approximation method reflects the actual conditions with a

1) L. Föppl: Report of the Meeting of the Bavarian Academy of Sciences 1921, Vol 51, p 41.
2) F. A. Willers: Dissertation, Göttingen. See also Ztschr. für Math. u. Phys. (Journal for Mathematics and Physics), Vol 55 (1907), p 225; A. Timpe: Math. Ann., Vol 71 (1911), p 480.
3) A. Föppl: VDI - Zeitschr. (Journal of the Association of German Engineers), 1900, p 1043.
4) F. A. Willers, Dissertation, Göttingen.

quite satisfactory accuracy, and hence we can consider the approximate solutions as being of a high quality, at least for those cases which alone are of practical importance.

1. Fundamentals of the Theory of Elasticity. A. Foppl[1] has demonstrated the truth of the following statement: If a solid of rotation having varying diameters is subjected to a torsion around its axis, then an elastic deformation will take place consisting of a distortion within the cross-sectional plane. This distortion is such that circles that have been drawn around the center of the cross section before the deformation remain circles also after deformation, but these circles of different diameters experience, in contrast to the cylindrical shaft itself, different angular displacements around the axis of rotation. This deformation has for consequence that only tangential shear stresses appear in the cross section, whereas the shear stresses in the longitudinal or meridional section are directed parallel and normal to the axis of rotation. Normal stresses appear neither in the cross section nor in the meridional sections. Due to the rotational symmetry of the state of deformation (and hence of stress), all meridional sections are equivalent, so that the stress conditions of the whole shaft are known as long as the two components of the shear stress in a meridional section are determined for each of its points. We choose the axis of rotation as the x-axis and denote the perpendicular distances from it by ρ. We call the axial shear-stress component τ_x, the radial component τ.

The equilibrium condition for an element of volume against dislocation in the tangential direction is

$$\frac{\partial \tau_x}{\partial x} + \frac{\partial \tau_\rho}{\partial \rho} + \frac{2\tau_\rho}{\rho} = 0 \quad \ldots\ldots\ldots \quad (1).$$

As is usual, we express the shear stress components by the elastic displacement v which takes place in the cross sectional plane, and its derivative, and eliminate from the two equations obtained in this way the displacement v. We then get the equation of compatibility

$$\frac{\partial \tau_x}{\partial \rho} - \frac{\partial \tau_\rho}{\partial x} - \frac{\tau_x}{\rho} = 0 \quad \ldots\ldots\ldots \quad (2).$$

Now, for the subsequent finding of approximate solutions, it is possible to express τ_x and τ as the differential quotients of a single function $F(x,\rho)$. This is so since, if we write

1) A. Föppl: VDI - Zeitschr. 1906, p 1032.

$$\tau_x = -\frac{1}{\varrho^2}\frac{\partial F}{\partial \varrho}; \quad \tau_\varrho = +\frac{1}{\varrho^2}\frac{\partial F}{\partial x} \quad \ldots\ldots\ldots \quad (3),$$

these values identically satisfy equation (1), and equation (2) transforms into

$$\frac{\partial^2 F}{\partial x^2} + \frac{\partial^2 F}{\partial \varrho^2} - \frac{2}{\varrho}\frac{\partial F}{\partial \varrho} = 0 \quad \ldots\ldots\ldots \quad (4).$$

The curves F = constant in the meridional section plane represent the stress curves, i.e., their direction at any point coincides with the direction of the stress transmitted there, as can be seen from the differential equation of these lines:

$$\frac{d\varrho}{dx} = -\frac{\frac{\partial F}{\partial x}}{\frac{\partial F}{\partial \varrho}} = +\frac{\tau_\varrho}{\tau_x} \quad \ldots\ldots\ldots \quad (5)$$

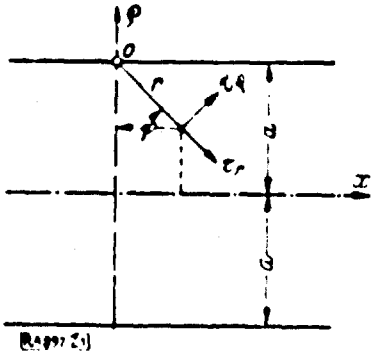

Fig. 1.

Since we have postulated that no external forces attack on the circumference of the shaft except on its ends, the shaft boundary itself, in the longitudinal section, represents a stress curve which we will denote by $\bar{F}$ = const.

The total torsional moment transmitted by the shaft of radius a is

$$M = 2\pi \cdot \bar{F} \quad \ldots\ldots \quad (6).$$

For the problems to be dealt with in the present paper it is advantageous to use polar coordinates, r, φ instead of the rectangular ones. We shall therefore transform the general equations given above into polar coordinates. The orientation of the polar coordinate system is shown in Fig. 1, representing the longitudinal section of a cylindrical shaft of radius a. We have

$$x = r \cdot \sin\varphi; \quad \varrho = a - r\cos\varphi,$$
$$\tau_\varrho = \tau_r \cdot \sin\varphi + \tau_\varphi \cos\varphi; \quad \tau_x = \tau_\varphi \sin\varphi - \tau_r \cdot \cos\varphi \quad \ldots\ldots \quad (7).$$

and thus, the equations (1) and (2) transform into

$$\frac{\partial \tau_r}{\partial r} + \frac{\tau_r}{r} + \frac{1}{r}\frac{\partial \tau_\varphi}{\partial \varphi} + 2\cdot\frac{\tau_\varphi \sin\varphi - \tau_r \cos\varphi}{a - r\cos\varphi} = 0 \quad \ldots\ldots \quad (1a),$$

$$\frac{1}{r}\frac{\partial \tau_r}{\partial \varphi} - \frac{\partial \tau_\varphi}{\partial r} - \frac{1}{r}\tau_\varphi - \frac{\tau_r \cdot \sin\varphi + \tau_\varphi \cdot \cos\varphi}{a - r\cdot\cos\varphi} = 0 \quad \ldots\ldots \quad (2a).$$

The stress components τ_r and τ_φ appear in the differential quotients of the stress function $F(r,\varphi)$ as follows:

$$\tau_r = \frac{1}{r}\cdot\frac{\partial F}{\partial \varphi}\cdot\frac{1}{(a - r\cdot\cos\varphi)^2};\quad \tau_\varphi = -\frac{\partial F}{\partial r}\cdot\frac{1}{(a - r\cos\varphi)^2} \qquad (3a),$$

as can be seen immediately if we substitute these values into equation (1a), which thus yields an identity.

A) The Symmetrical Problem

2. The Cylindrical Shaft Completely Surrounded by a Semicircular Groove. (See Fig. 2 showing that part of the longitudinal section lying above the axis.) We start from the stress function of the smooth cylindrical shaft which in the polar coordinates (Fig. 1) used here reads as follows:

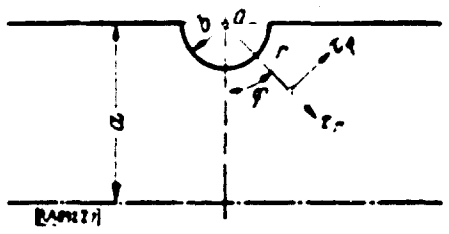

Fig. 2.

$$F = C\cdot(a - r\cos\varphi)^4 \qquad (8),$$

where C is a constant. F = 0 on the shaft axis, i.e., for $r = \frac{a}{\cos\varphi}$, and $\overline{F} = Ca^4$ on the boundary, i.e., for $\cos\varphi = 0$. Considering eq. (6) it follows that

$$C = \frac{M}{2\pi\cdot a^4} \qquad (9),$$

Denoting the groove radius by b, we expand the equation for the stress function of the smooth cylindrical shaft, eq. (8), and so obtain, as the simplest imaginable approximation formula for the stress function of a grooved shaft:

$$F = C\cdot\left[a - r\cdot\left(c_1\cdot\left(\frac{b}{r}\right)^m + c_2\cdot\left(\frac{b}{r}\right)^n + 1\right)\cos\varphi\right]^4 \qquad (10),$$

where m and n are two as yet undertermined positive numbers. The solution of the problem depends on their appropriate designation. For b = 0 and $r = \infty$, this expression transforms into eq. (8), as it should. Coefficients c_1 and c_2 are obtained from the two limiting conditions:

$$1.\ F = C\cdot a^4 \text{ FOR } r = b;\quad 2.\ F = 0 \text{ FOR } r = \frac{a}{\cos\varphi} \qquad (10a).$$

The third limiting condition, according to which F must become $C \cdot a^4$ on the boundary outside the groove, is automatically satisfied. According to eq. (6), the constant C becomes $C = \frac{M}{2\pi a^4}$. If we introduce as an abbreviation $\frac{b \cdot \cos \varphi}{a} = y$, then it follows from the two limiting conditions of (10a) that

$$c_1 = \frac{n}{y^m - y^n}; \quad c_2 = -(c_1 + 1) \quad \ldots \ldots \ldots \quad (11).$$

If, for the sake of brevity, we substitute w for the term between the brackets of eq. (10) we obtain for the stress components:

$$\tau_r = + \frac{4 C \cdot w^3}{(a - r\cos\varphi)^3} \left\{ \left[c_1 \left(\frac{b}{r}\right)^m + c_2 \left(\frac{b}{r}\right)^n + 1 \right] \sin\varphi - \left[\frac{\partial c_1}{\partial \varphi} \left(\frac{b}{r}\right)^m + \frac{\partial c_2}{\partial \varphi} \left(\frac{b}{r}\right)^n \right] \cos\varphi \right\} \quad (12),$$

$$\tau_z = - \frac{4 C \cdot w^3}{(a - r\cos\varphi)^3} \left[c_1 (m+1) \left(\frac{b}{r}\right)^m + c_2 (n+1) \left(\frac{b}{r}\right)^n + 1 \right] \cos\varphi \quad \ldots \quad (13).$$

The stress of main interest is τ_φ. Its maximum lies at the bottom of the groove, i.e., for r = b, φ = 0. At this point, as everywhere else on the boundary, w = a, so that

$$(\tau_\varphi)_{\substack{r=b \\ \varphi=0}} = \frac{4 C \cdot a^3 [c_1 (m+1) + c_2 (n+1) + 1]}{(a-b)^3} \quad \ldots \ldots \quad (14).$$

The quantities m and n could hitherto assume any arbitrary positive value. To determine them, we use the condition that $(\tau_\varphi)_{\substack{r=b \\ \varphi=0}}$ becomes twice the value of the circumferential stress of the smooth cylindrical shaft of radius a, when the groove radius becomes infinitesimally small. This was shown by Willers[1] (approximately) and by L. Föppl[2] (rigorously, by means of the Bessel functions). The rigorous proof of this stress duplication, known as "notch effect," will be shown here in still another manner.

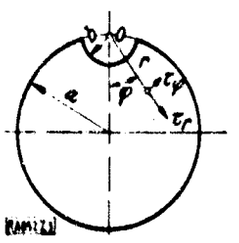

Fig. 3.

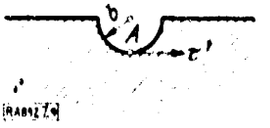

Fig. 4.

We first consider a torsion problem, completely different from that at hand, but one for which it is possible to find a rigorous solution, namely the problem of a cylindrical shaft

1) See Willers, loc. cit., page 251.
2) L. Föppl: Report of the Meeting of the Bavarian Academy of Sciences, 1921, Vol 51, page 61.

weakened by a semicircular key groove, running parallel to the axis (Fig. 3). We assume the radius b of the keyway to be negligibly small compared with shaft radius a. Moreover, we consider only that part of the shaft's cross section that is in the immediate vicinity of the keyway and is represented in Fig. 4 in infinite magnification. We proceed analogously with the grooved shaft, which is also represented by Fig. 4, if we consider this figure to be a part of the longitudinal section of this shaft. If we assume the shaft radius and the torsional moment to be equally large in both cases, then the tangential stresses τ_0 of both shafts, at a sufficiently large distance from the semicircle, are also equal. The stress lines can be considered by hydrodynamic analogy as the streamlines of a plane fluid motion that flows through the cross section or longitudinal section, respectively. We denote the velocity vector in the cross section of the shaft with the keyway by s_1, the velocity vector in the longitudinal section of the grooved shaft by s_2, and the shear stresses accordingly by τ_1 and τ_2. In order for the fluid motions to remain free of poles the following relations must exist between s and τ, as is well known:

$$s_1 = p \cdot \tau_1, \qquad s_2 = q \cdot \rho^2 \cdot \tau_2 \qquad (15),$$

where p and q are arbitrary factors of proportionality and ρ is, as before, the distance of a point on the longitudinal section from the shaft axis. On the circumference of the shaft, at a sufficiently great distance from the keyway or the neck respectively, and with $\rho = a$, we have:

$$(s_1)_0 = p \cdot (\tau_1)_0 = p \cdot \tau_0, \qquad (s_2)_0 = q \cdot a^2 (\tau_2)_0 = q \cdot a^2 \cdot \tau_0 \qquad (16).$$

s and τ assume their maximum values s_1', τ_1', and s_2', τ_2', respectively at point A (Fig. 4). Since here b becomes negligibly small compared with a, we have to write $\rho = a$, in this case too, and

$$s_1' = p \cdot \tau_1', \qquad s_2' = q \cdot a^2 \cdot \tau_2' \qquad (17).$$

We see immediately from eq. (16) and (17) that with $p = q \cdot a^2 = 1$ both flows become identical in the boundary regions, i.e., we have:

$$s_1 = s_2 = s = \tau \qquad (18),$$

whence

$$\tau_1' = \tau_2' = \tau' \qquad (19)$$

We shall subsequently prove that if the stress increase τ'/τ_0 caused by the notch effect can be found for one case, it is

known at the same time also for the other case. We can moreover deduce from this consideration that the stress increase will have about the same magnitude in both cases even at finite values of b, as long as they are small compared with a.

Denoting the stress function by f the rigorous solution for the shaft with a semicircular keyway[1] (circular-arc moonlet) (Fig. 3) is in polar coordinates

$$f = (2a\cos\eta - r)\left(\frac{r}{b} - \frac{b}{r}\right)b \cdot \frac{G\cdot\vartheta}{2} \qquad (20)$$

where ϑ is the torsion angle. The function f satisfies the limiting conditions, because it disappears on the edge of the cross section (for r = 2a cos y and for r = b) and also satisfies also the compatibility equation:

$$\frac{\partial^2 f}{\partial r^2} + \frac{1}{r}\frac{\partial f}{\partial r} + \frac{1}{r^2}\cdot\frac{\partial^2 f}{\partial \eta^2} = -2G\cdot\vartheta \qquad (21)$$

as can easily be seen by substituting into it f of eq. (20). The stresses are obtained in the usual manner and are

$$\tau_z = a\cdot\sin\eta\left(1 - \frac{b^2}{r^2}\right)G\cdot\vartheta, \qquad \tau_z = -\left(a\cos\eta - r + \frac{a\cdot r^2}{r^2}\cos\eta\right)G\vartheta \qquad (22)$$

If we substitute here for τ_m : r = b and φ = 0, and also b = 0, we obtain for the stress sought which we designated before as τ' the value $\tau' = 2a\cdot G\cdot\vartheta$. Since b = 0, the respective torsion angle ϑ for the smooth cylindrical shaft is, $\vartheta = \frac{2M}{G\pi a^4}$; thus: $\tau' = 2\cdot\frac{2M}{\pi\cdot a^2} = 2\,\tau_o$, which proves the stress duplication due to the notch effect also for the shaft with the neck groove.

Setting this value of τ' equal to the right side of eq. (14), in which b is made equal to 0, we obtain a condition equation for quantities m and n. This equation with $C = \frac{M}{2\pi a^4}$, and considering that $c_2 = -(c_1 + 1)$, is

$$(c_1)_m = 0\,(m - n) - n + 2 = 0 \qquad (33).$$

1) This solution was found by the author quite some time ago and was confirmed, among other proofs, experimentally by means of a Prandtl tension loop produced by a soap film. Meanwhile it was also given by C. Weber. See Forsch.-Arbeiten [Research Papers] No 249, page 31.

According to eq. (11) we first get for $(c_1)_{b=0}$ the indeterminate form 0/0. The true value is found if we differentiate both numerator and denominator with respect to y, it is

$$(c_1)_{b=0} = \frac{n}{m \cdot (y)_{b=0}^{m-n} - n} \quad \ldots \ldots \ldots \quad (24).$$

Since the quantities m and n must necessarily be positive, integer or fractional, numbers which are different from each other, we have with m > n:

$$(c_1)_{b=0} = -1 .$$

Substituting this value into eq. (23), n cancels out, and we obtain

$$m = 2 \quad \ldots \ldots \ldots \ldots \quad (25).$$

To obtain unknown n, whose value must in any case be equal to or larger than zero and smaller than 2, one could utilize the principle of the minimal deformation energy, but this proves unfeasible here, because the calculation becomes far too complicated. But various reasons, among others also the analogy with the shaft with the keyway (see footnote 1) on page 11 [of this manuscript]) indicate that we must take for n, here as well as there, the smallest permissible value, i.e., the value which differs most from m. Incidentally, as we saw before for a vanishing, small b, the value of n is arbitrary within the permissible limits, hence the choice of a specific value for n is practically of minor importance in the case of small groove radii. We shall thus put n = 0 and we shall see that this leads to a very good agreement with the results of Willers. Collecting the terms, the now completely determined stress function reads:

$$F = \frac{M}{2\pi \cdot a^4}\left[a - \frac{a^2 \cos\varphi}{(a^2 - b^2\cos^2\varphi)} \cdot \frac{(r-b)^2}{r}\right]^4 = \frac{M}{2\pi \cdot a^4} \cdot w^4 \quad \ldots \quad (26).$$

The stress component τ_φ, which is of main interest, becomes

$$\tau_\varphi = \frac{2M \cdot w^3 \cdot (r^2 + b^2) \cdot \cos\varphi}{\pi \cdot a^2 \cdot r^3 \cdot (a - r\cos\varphi)^2 (a^2 - b^2\cos^2\varphi)} \quad \ldots \ldots \quad (27).$$

It is worth noting that this expression rigorously satisfies the compatibility equation eq. (2a) along the semicircular boundary line on which τ_r and $\frac{\partial \tau_r}{\partial \varphi}$ disappear, if the transition radius b becomes infinitesimally small.

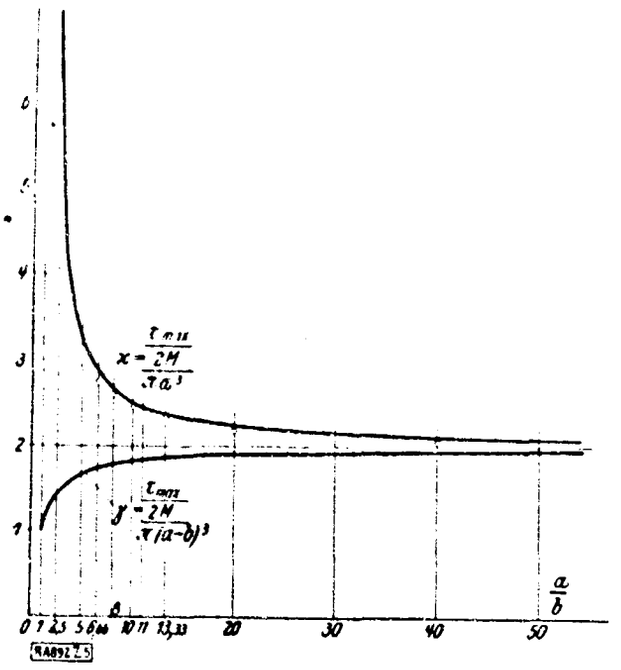

Fig. 5.

For r = b we obtain

$$(\tau_\varphi)_{r=b} = \frac{2M}{\pi \cdot (a - b\cos\varphi)^3} \cdot \frac{2a\cos\varphi}{(a + b\cos\varphi)} = \frac{2M}{\pi a^3} \cdot \frac{2a^4\cos\varphi}{(a - b\cos\varphi)^3 (a + b\cos\varphi)} = \frac{2M}{\pi a^3} \cdot \beta_1 \quad (28).$$

For the maximum stress at the bottom of the groove, i.e., at the boundary point $\varphi = 0$, we get the simple formula

$$\tau_{max} = (\tau_\varphi)_{\substack{r=b \\ \varphi=0}} = \frac{2M}{\pi \cdot (a-b)^3} \cdot \frac{2a}{(a+b)} = \frac{2M}{\pi (a-b)^3} \cdot \gamma \quad \ldots \quad (29).$$

The first factor represents that maximum stress which would result if we assumed a linear stress distribution in the cross section $\varphi = 0$; the second factor γ characterizes the stress increase. Fig. 5 shows the proportionality values $\frac{\tau_{max}}{\frac{2M}{\pi a^3}} = \chi$ and $\frac{\tau_{max}}{\frac{2M}{\pi (a-b)^3}} = \gamma$ as functions of a/b in graphical form, whereas the values found by Willers are indicated by small circles. The agreement is very satisfactory. Table 1 shows the computed results of the proportionality values for a number of a/b values. The stress component τ_r becomes

$$\tau_r = \frac{2M w^2 \sin\varphi\,(r^2 - b^2)\,(a^2 + b^2\cos^2\varphi)}{\pi \cdot (a - r\cos\varphi)^3 a^3 \cdot r^3 (a^2 - b^2\cos^2\varphi)^2} \quad (30).$$

TABLE 1.

$\tau_{max} = \frac{2M}{\pi \cdot a^3} \cdot \varkappa$, $\tau_{max} = \frac{2M}{\pi \cdot (a-t)^3} \cdot \gamma$, (1) vergl. Abb. 5

$\frac{a}{b}$	1	2,5	5	6,66..	8	10	11	13,33.	20	30	40	50	∞
$\varkappa$ (2)	∞	6,6	3,25	2,84	2,64	2,49	2,44	2,36	2,22	2,15	2,10	2,09	2,0
$\varkappa$ (nach Willers)	∞	--	3,07	2,76	2,60	2,46	—	2,33	2,17	—	2,04	—	2,0
$\frac{\varkappa - \varkappa_w}{\varkappa_w} \cdot 100$	—	—	+5	+3	+2	+1,5	—	+1	+2	—	+3	—	0
γ	1	1,13	1,67	1,71	1,78	1,82	1,835	1,86	1,9	1,985	1,95	1,98	2

1 -- See Fig. 5; 2 -- (according to Willers).

On the generatrix outside the groove, i.e., for $\varphi = \pi/2$, $(\tau_\varphi)_{\varphi=\pi/2} = 0$ and the boundary stress[1] becomes

$$(\tau_r)_{\varphi=\pi/2} = \frac{2M}{\pi a^3}\left[1 - \left(\frac{b}{r}\right)^3\right] = \frac{2M}{\pi \cdot a^3}\beta_3 \quad \ldots\ldots\ldots \quad (31).$$

For $r = \infty$, or for $b = 0$, this value transforms into that valid for the circumferential stress of the smooth cylindrical shaft. At the corners $r = b$, $\varphi = \pi/2$, both τ_r and τ_φ disappear. The stress in the weakest cross section obeys the law:

$$(\tau_\varphi)_{\varphi=0} = \frac{2M(a^3\varphi \ldots 0(r^3 + b^3)}{\pi \cdot a^2 \cdot r^3 \cdot (a-r)^2 (a^3 - b^3)} = \frac{2M}{\pi \cdot (a-b)^3} \cdot \gamma_1 \quad \ldots\ldots \quad (32).$$

Fig. 6 shows, for the case $a/b = 11$, the functions for the boundary stresses $(\tau_\varphi)_{r=b}$ and $(\tau_r)_{\varphi=\pi/2}$, as well as the stress in the weakest cross section $(\tau_\varphi)_{\varphi=0}$ in graphical form. The corresponding numerical values are given in Tables 2 through 4. We see from the stress distribution over the weakest cross section that the torsional moment is transmitted mainly by the outer layers of the shaft, while the layers closer to the axis carry less of the load[2].

1) Willers, too, arrives at this equation on page 254 of his paper by means of an approximate integration of the differential equation for the case that b is very small compared to a.

2) The deductions drawn from the hydrodynamic analogy lead also to a certain similarity between the grooved shaft and the shaft having the keyway, in regard to the stress distribution in the border regions. Since our formula for F worked out well in the case of the grooved shaft, it seemed feasible

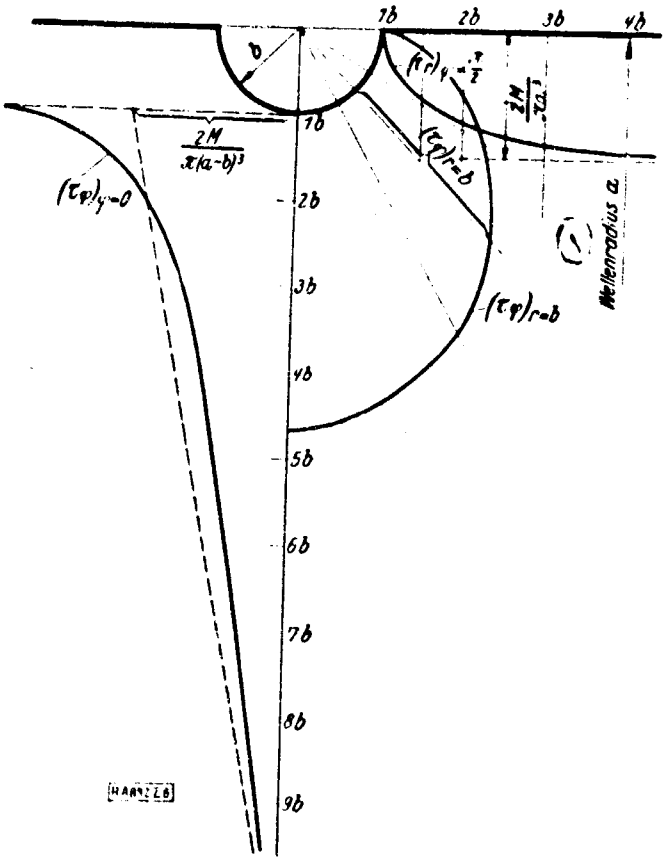

Fig. 6.
1 -- Shaft radius a.

---

to try an equation for the stress function of the shaft with the keyway, developed exactly like eq. (10), and then to compare its results with those obtained by the rigorous solution. This equation, using the notations of Fig. 3, is

$$F = \frac{\sigma \cdot \vartheta}{2} \cdot r \cdot \left[2a\cos\varphi - r \cdot \left(C_1 \cdot \left(\frac{b}{r}\right)^m + C_2 \cdot \left(\frac{b}{r}\right)^n + 1\right)\right],$$

which changes over into the expression for the full circle if b = 0. The limiting conditions here are F = 0 for r = b and r = 2a cos φ and it follows from the condition of the doubling of the stress due to the notch effect, that m = 3; we cannot state at first anything about n, except that it certainly is < 3. To determine n, there is at our disposal the additional condition that the stress must disappear in the center of the cross section; this center coincides with the shearing center (and not, as one could think, with the center of gravity). This condition yields for n very exactly the value 0. We thus obtain for the stress on the radius vector φ = 0:

$$(\tau_\varphi)_{\varphi=0} = \frac{\sigma \cdot \vartheta}{2}\left[2a + (C_1)_{\varphi=0}\frac{b^3}{r^2} - 2r \cdot ((C_2)_{\varphi=0} \cdot b + 1)\right].$$

The behavior of the border stress $(\tau_r)_{\varphi=\pi/2}$ on the cylindrical part of the shaft, represented in eq. (31) has been tested in experiments and well confirmed. (See also the test report.) The a/b of the test shaft was 11. According to Table 1, the stress increase at the bottom of the groove is 83.5%. The disturbance in the stress distribution of the cylindrical shaft, caused by the turned-in groove, practically disappears at a distance of 10b, measured axially from the pole.

TABLE 2.

$(\tau_\varphi)_{r=b} = \frac{2M}{\pi \cdot a^3} \cdot \beta_1$, (1) für den Fall: $\frac{a}{b} = 11$, (2) vergl. Abb. 6

φ	0^0	30^0	45^0	60^0	90^0
β_1	2,44	2,05	1,62	1,1	0

1 -- For the case; 2 -- See Fig. 6.

TABLE 3.

$(\tau_r)_{\varphi=\pi/3} = \frac{2M}{\pi \cdot a^3} \cdot \beta_2$, (1) für den Fall: $\frac{a}{b} = 11$, (2) vergl. Abb. 6

$\frac{r}{b}$	1	1,2	1,4	1,6	1,8	2,0	3	4	5	10
β_2	0	0,805	0,49	0,61	0,69	0,75	0,89	0,945	0,96	0,99

1 -- For the case; 2 -- See Fig. 6.

where the following holds true if we use the abbreviation $\frac{b}{2a\cos\varphi} = z$:

$$a_1 = \left(\frac{\varepsilon - 1}{\varepsilon}\right) \cdot \frac{1}{z^3 - 1}, \qquad a_2 = \frac{1 - \varepsilon}{\varepsilon} - a_1$$

The numerical evaluation yields an extremely close approximation to the stress distribution of the rigorous solution, even when the ratio b/a has rather higher values. The deviations in the maximum stress e.g., for b/a = 1/3 are about -3%, and the deviations of the torsion angle about +6%. The approximation used here thus yields a high quality approximate solution also for this torsion problem.

TABLE 4.

$(\tau_\varphi)_{\varphi=0} = \frac{2M}{\pi (a-b)^3} \cdot \gamma_1$. (1) für den Fall: $\frac{a}{b} = 11$. (2) vergl. Abb. 6

$\frac{r}{b}$	1	2	3	4	5	7	8	9	11
γ_1	1,835	0,902	0,684	0,541	0,466	0,304	0,221	0,189	0

1 -- For the case; 2 -- See Fig. 6.

3. Shaft with Concentric Hole and Turned-in Groove. If g is the radius of the axial drill hole, then depression F, already modified for the limiting conditions of 1) $\overline{F} = Ca^4$ for $r = b$; 2) $\overline{F} = C \cdot g^4$ for $r = \frac{a-g}{\cos \varphi}$, is:

$$F = \frac{M}{2\pi (a^4 - g^4)} \left[a^4 - \frac{(r^2 - b^2)(a-g)^3 \cos \varphi}{(a-g)^3 - b^3 \cos^3 \varphi} \right]^4 \quad \ldots \quad (33).$$

For the maximum stress we obtain

$$\tau_{max} = \frac{2M(a-b)}{\pi \cdot [(a-b)^4 - g^4]} \cdot \frac{2a^3 [(a-b)^4 - g^4] (a-g)^3}{(a^4 - g^4)(a-b)^3 [a-g)^3 - b^3]} \quad \ldots \quad (34),$$

where the second factor represents the stress increase over a linear distribution.

On the shaft circumference outside the groove we have

$$(\tau_\varphi)_{r=b,\varphi=\pm\frac{\pi}{2}} = \frac{2M}{\pi \cdot (a^4 - g^4)} \left(1 \quad \left(\frac{b}{r}\right)^3\right) \quad \ldots \quad (35).$$

The stress in the weakest cross section ($\varphi = 0$) is distributed according to the following law:

$$(\tau_\varphi)_{\varphi=0} = \frac{2M \cdot a}{\pi \cdot (a^4 - g^4)} \cdot \frac{w \cdot a^3 + b^3)(a-g)^3}{(a-r)^3 \cdot r^3 [(a-g)^3 - b^3]} \quad \ldots \quad (36).$$

w denotes the expression within brackets of equation (33).

The stress increase for the case of $\frac{a}{b} = 11$, $\frac{a}{g} = \frac{11}{3}$ is 84% (as compared with 83.5% for the shaft without the bore hole).

4. Shaft with a Slot-Like Turned-In Groove Whose Depth is Larger than the Transition Radius (Fig. 7). Here, the general form of the stress function is derived in the same manner as in Section 2. It is

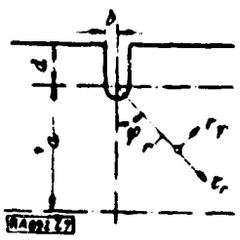

Fig. 7.

$$F = K \cdot [a - r \cdot (g_1 \left(\frac{b}{r}\right)^2 + g_2) \cos \varphi]^4$$

Here the constant K, using notations of Fig. 7, is $K = \frac{M}{2\pi \cdot (a+d)^4}$, while the coefficients g_1 and g_2 are found from the limiting conditions. The limiting conditions in the region of the longitudinal section of the shaft between axis and radius vector $\varphi =$ $= \pi/2$: $F = 0$ for $r = \frac{a}{\cos \varphi}$ and $\overline{F} = K \cdot (a + d)^4$ for $r = b$. We find

$$g_1 = -\frac{a^2\left(1 + \frac{d}{b \cos \varphi}\right)}{a^2 - b^2 \cos^2 \varphi}, \qquad g_2 = \frac{a^2 + b\,d \cdot \cos \varphi}{a^2 - b^2 \cos^2 \varphi}$$

therefore

$$F = \frac{M}{2\pi (a+d)^4}\left[a + \frac{a^2 \cdot \frac{b}{r}(b \cos \varphi + d) - r \cos \varphi (a^2 + b\,d \cos \varphi)}{a^2 - b^2 \cos^2 \varphi}\right]^4 = \frac{M}{2\pi \cdot (a+d)^4} \cdot u^4 \quad (37)$$

and

$$\tau_\varphi = -\frac{1}{(a - r \cos \varphi)^3} \cdot \frac{\partial F}{\partial r} = \frac{2M \cdot u^3}{\pi \cdot (a+d)^4 (a - r \cos \varphi)^3} \cdot \frac{\frac{a^2 b}{r^3}(b \cos \varphi + d) + \cos \varphi (a^2 + b\,d \cos \varphi)}{a^2 - b^2 \cos^2 \varphi} \quad (38)$$

In particular, we obtain for the stress distribution law in the weakest cross section

$$(\tau_\varphi)_{\varphi=0} = \frac{2M}{\pi \cdot (a-b)^3} \cdot \frac{(u)^3_{\varphi=0} = u(a \quad b)^3\left[\frac{a^2 \cdot b}{r^3}(b + d) + a^2 + b\,d\right]}{(a+d)^4 \cdot (a \quad)^3 \cdot (a+b)} \quad . \quad . \quad (39),$$

from which the maximum stress at the bottom of the groove is found

$$\tau_{max} = (\tau_\varphi)_{\substack{\varphi=0 \\ r=b}} = \frac{2M}{\pi \cdot (a-b)^3} \cdot \frac{\frac{a^2}{b}(b + d) + a^2 + b\,d}{(a+b)(a+d)} = \frac{2M}{\pi \cdot (a-b)^3} \cdot \nu \quad (40).$$

Factor ν signifies how much the stress is increased when compared with the linear stress distribution in the weakest cross section. Taking $d = 0$ (case of the semicircular groove) ν becomes $\nu = \frac{2a}{a+b}$, as it should be according to eq. (29).

For b = 0, i.e., for the case of an infinitesimally narrow slot, we have $\nu = \infty$. On the radius vector $\varphi = \pi/2$ we obtain

$$(\tau_\varphi)_{\varphi=\pi/2} = \frac{2M\cdot\left[a + r\cdot\frac{d}{b}\left(\frac{b}{r}\right)^2\right]^2}{\pi\cdot(a+d)^4\cdot a^3}\cdot\frac{d}{b}\cdot\left(\frac{b}{r}\right)^3 \quad . \quad . \quad . \quad . \quad . \quad (41)$$

and:

$$(\tau_r)_{\vartheta=\pi/2} = \frac{2M\cdot\left[a + r\cdot\frac{d}{b}\cdot\left(\frac{b}{r}\right)^2\right]^2}{\pi\ (a+d)^4\ a^3}\cdot\left[1-\left(\frac{b}{r}\right)^2\right] \quad . \quad . \quad . \quad . \quad (42).$$

From this we can compute the variable angle ϑ, at which the radius vector $\varphi = \pi/2$ is intersected by the stress lines running parallel to the axis, at a large distance from the slot and above this radius vector. This angle is found from

$$\operatorname{tg}\vartheta = \left(\frac{\tau_\vartheta}{\tau_r}\right)_{\varphi=\pi/2} = \frac{d\cdot b}{r^2 - b^2} \quad . \quad . \quad . \quad . \quad . \quad . \quad . \quad (43).$$

To visualize how the stress lines crowd together in the vicinity of the groove bottom, we can e.g., calculate the coordinate r_o of the point at which the radius vector $\varphi = 0$ is intersected by the stress line which coincides, at a large distance from the slot, with the radius vector $\varphi = \pi/2$. We take for this purpose $(w)_{\substack{\varphi=\pi/2 \\ r=\infty}} = a = (w)_{\varphi=0}$ and find from it

$$r_o = b\cdot\sqrt{\frac{1+\frac{d}{a}}{\frac{a}{a}+\frac{d}{a}}} \quad (44)$$

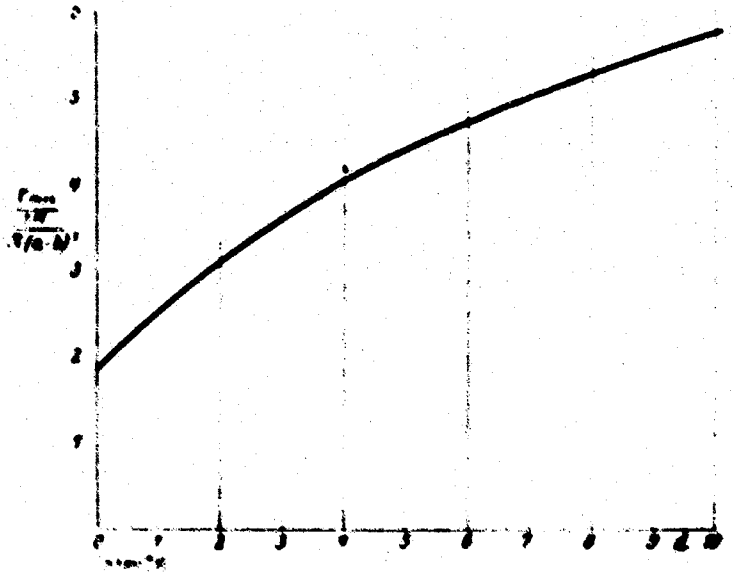

Fig. 8.

In this way we obtain e.g., for the case where a = 11 cm, b = = 1 cm, d = 4 cm, a value of r_o = 2.2 cm. Using the illustrative hydrodynamic analogy, this means that the fluid which flows in a ribbon of 4 cm width, at a large distance from the slot and above the radius vector $\varphi = \pi/2$, now occupies a width of only 1.2 cm when it passes the radius vector $\varphi = 0$. Fig. 10 depicts this numerical example. It shows several stress lines and their tangents where they intersect the radius vector $\varphi = \pi/2$. The curve of Fig. 8 shows the stress increases, which follow from eq. (40) for the case $\begin{cases} a = 11 \\ b = 1 \end{cases}$ as a function of d. The corresponding numerical values are given in Table 5 which also shows the ratio between the boundary stresses at the border point $\varphi = \pi/2$ and the corresponding maximum stresses. Fig. 9 and Tables 6 and 7 show the stress distribution in the weakest cross section according to eq. (39) for the case of a/b = 11, $\frac{a - b}{d} = 2.5$. They also show the behavior of the boundary stress along the circular borderline. Finally, Fig. 10a and Table 7a show graphically and numerically the factor ν as a function of b for the case a = 11, d = 4. This factor characterizes the stress increase.

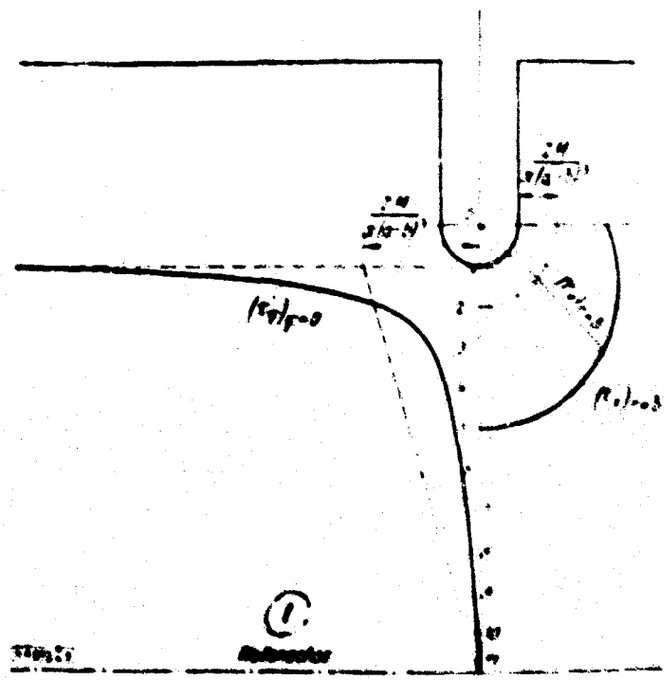

Fig. 9.

1 -- Shaft Axis.

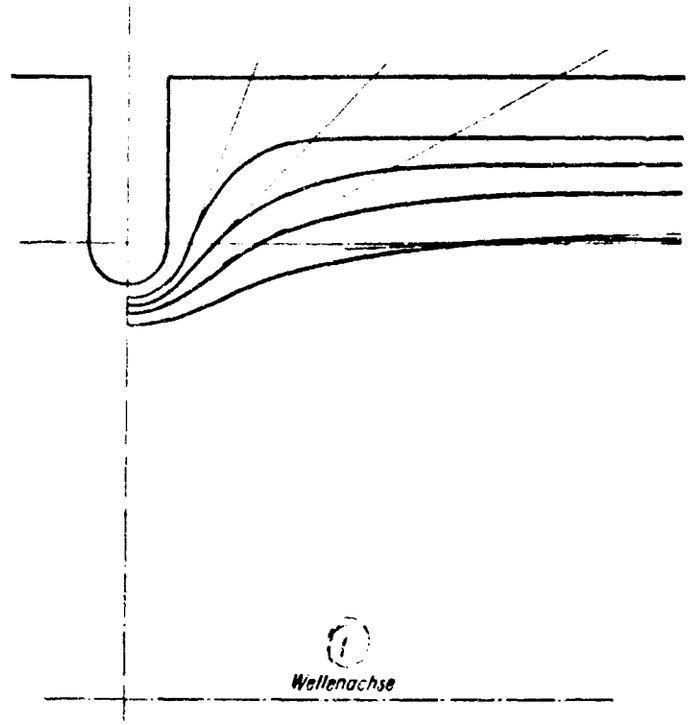

Fig. 10.

1 -- Shaft Axis.

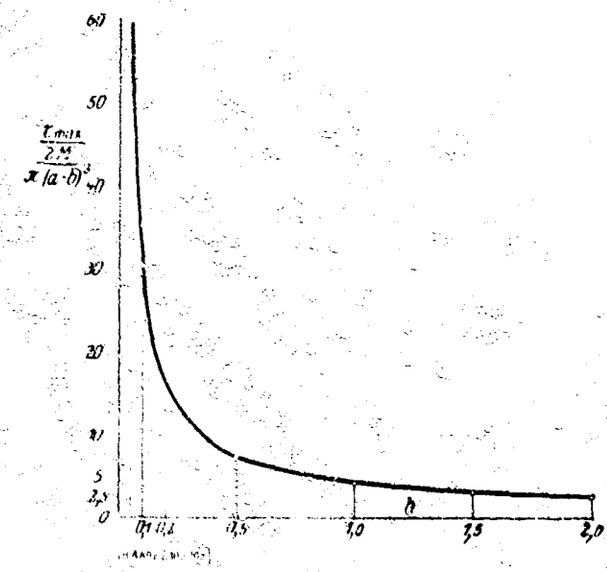

Fig. 10a.

Willers did not investigate this problem, hence the formulae derived here can be tested only indirectly by the results of Section 7 below. We state right now that a good agreement with Willers' values is obtained. We shall not pursue here the stress distribution in the region of the longitudinal section above the radius vector $\varphi = \pi/2$, since it is of only minor interest.

TABLE 5.

$\tau_{max} = \frac{2M}{\pi \cdot (a-b)^3} \nu$, für den Fall: $a = 11$, $b = 1$, vergl. hierzu Abb. 8

d	0	1	2	3	4	5	10	∞
ν	1,83	2,53	3,11	3,62	4,06	4,43	5,80	10,16
$\frac{(\tau_\varphi)_{r=b}}{\tau_{max}}$	0	0,273	0,408	0,489	0,544	0,583	0,678	0,814

1 -- For the case; 2 -- See also Fig. 8.

TABLE 6.

$(\tau_{\varphi})_{r=b} = \frac{2M}{\pi \cdot (a-b)^3} \cdot \varkappa_1$, für den Fall: $\frac{a}{b} = 11$, $\frac{a-b}{d} = 2{,}5$, vergl. hierzu Abb. 9

$\frac{r}{b}$	1	1,5	2	3	4	5	6	8	11
$\varkappa_1$	4,06	1,51	0,84	0,43	0,29	0,21	0,15	0,09	0

1 -- For the case; 2 -- See also Fig. 9.

TABLE 7.

$(\tau_{\varphi})_{r=b} = \frac{2M}{\pi \cdot (a-b)^3} \varkappa_2$, für den Fall $\frac{a}{b} = 11$, $\frac{a-b}{d} = 2.5$, vergl. Abb. 9

φ	0^0	30^0	45^0	60^0	90^0
$\varkappa_2$	4,06	3,76	3,43	3,08	2,22

1 -- For the case; 2 -- See also Fig. 9.

The case of the shaft with a concentric bore hole can be dealt with as before without difficulty.

B) The Assymetrical Problem

5. Stepped Shaft Whose Step Height Equals the Transition Radius (Fig. 11). This problem, as well as that discussed in the next section, is of special importance from the point of view of practical application, because the stepped shaft belongs to the machine parts most frequently used in machine design.

TABLE 7a.

$\tau_{max} = \frac{2M}{\pi \cdot (a-b)^3}$, (1) für den Fall: $a = 11$, $d = 4$, (2) vergl. hierzu Abb. 10a

b	0	0,05	0.1	0,2	0,5	1.0	1,5	2.0
ν	∞	59,9	30,5	15.1	7,03	4,06	3,05	2,52
$\frac{(\tau_\varphi)_{r=b,\ \varphi=\pi/2}}{\tau_{max}}$	1	0,788	0.721	0.694	0.626	0,542	0.482	0.437

1 -- For the case; 2 -- See also Fig. 10a.

We call the small step "half notch," to distinguish it from the "full notch," which corresponds to a small semicircular groove. In the present case of the half notch, the limit of the factor characterizing the stress increase in the borderpoint $\varphi = 0$, is, for an infinitesimally small transition radius, obviously 1.5 (average of numbers 2 and 1 which are respectively applicable to the full notch and the smooth shaft). This can be proved in detail by a somewhat cumbersome calculation, which however we omit here for the sake of brevity. Here eq. (14) is valid without changes and it thus follows that $m = 1.5$. But we try to avoid fractional exponents in the interest of arriving at formulae that are conveniently evaluated numerically. We shall therefore introduce this limit into the calculation in another way, which leads to a practically complete agreement with Willers' results. Introducing the new coefficients e_1 and e_2, and with $m = 2$ and $n = 0$, the equation (10) now reads

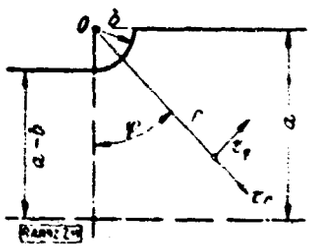

Fig. 11.

$$F = C \cdot [a - r \cdot (e_1 \cdot \left(\frac{b}{r}\right)^2 + e_2) \cos \varphi]^4 \quad \ldots\ldots\ldots \quad (45).$$

The boundary condition for $r = b$ demands that $e_2 = -e_1$, we can therefore write

$$F = C \cdot [a - r \cdot e_1 \left(\frac{b}{r} - 1\right) \frac{r+b}{r} \cos \varphi]^4 \quad \ldots\ldots\ldots \quad (46).$$

From this the maximum stress for the grooved shaft is obtained as

$$\tau_{max} = (\tau_\varphi)_{\substack{r=b \\ \varphi=0}} = \frac{4\,C\,a^3}{(a-b)^3} e_1 \cdot \left(\frac{r+b}{r}\right)_{r=b} \quad \ldots\ldots\ldots \quad (46a).$$

where the term in parentheses means the limiting value of the stress increase for infinitesimally small groove radius b (on account of $(e_1)_{b=0} = -1$). Adding to the numerator and the denominator of this expression the quantity b, the expression assumes the value 1.5 according to the prescription for r = b applying in this case and the results obtained by this simple means differ only very slightly from those which we would have obtained with m = 1.5. These considerations suffice also to determine the border stress at point $\varphi = 0$. This stress can be considered as the maximum stress, as will be shown later and as it follows also from Willers' paper. The simple calculation which proceeds analogously to that of Section 2, yields for this stress the extremely simple formula

$$\sigma_{\varphi}\Big)_{\substack{r=b\\ \varphi=0}} \cong \sigma_{max} = \frac{2M}{\pi a^3 b^3} \cdot \frac{3}{2} \cdot \frac{a+b}{a+2b} = \frac{2M}{\pi (a-b)^3} \cdot \lambda_1 \quad . \quad . \quad . \quad . \quad (47)$$

If however we raise the question of the stress distribution in the longitudinal section of the shaft and of the magnitude and the location of the real maximum stress, then the expression in parentheses of the stress function must be expanded by a term which is odd in φ, on account of the asymmetrical course of the stress lines with respect to the radius vector $\varphi = 0$, which is obviously no longer intercepted by them at a right angle, except by the border line. The stress function can now be written:

$$F = \frac{M}{2\pi a^4} \cdot \left[a^4 \cdot r^4 \cdot \varrho_1 \left(\frac{b}{r} - 1 \right) \left\{ \frac{r+2b}{r+b} \cos \varphi + f(r) \sin 2\varphi \right\} \right]^4 = \frac{M}{2\pi \cdot a^4} \cdot z^4 \quad (48),$$

where the double angle in the sine term stems from the limiting condition: $\overline{F} = C \cdot a^4$ for the border $\varphi = \pi/2$. This term must in any case disappear at point $\varphi = 0$, since the stress increase at this point follows already from the symmetrical part of the stress function discussed above.

About the function f(r) we can only state that it must disappear for b = 0 and decay rapidly with increasing r. Theoretical considerations could provide no further information on the shape of this function, so we resorted to experiments to determine it approximately, with good success. If we take

$$f(r) = + \left(\frac{b}{r+b} \right)^3 \quad . \quad . \quad . \quad . \quad . \quad . \quad . \quad . \quad . \quad (49),$$

we achieve a very satisfactory agreement between the calculated and measured border stresses along the cylindrical parts of the shaft.

Omitting the auxiliary calculations, we obtain from eq. (48) in the usual manner

$$\tau_z = \frac{2M}{\pi a^3} \cdot \frac{s^3 (a + b\cos\varphi) \cdot \left[(r^2 + 2rb + 3b^2)\cos\varphi + \frac{3b^3 - r \cdot b^2}{r + b} \sin 2\varphi\right]}{(a - r\cos\varphi)^3 (a - b\cos\varphi) \cdot \left[a + b\cos\varphi \left(2 + \frac{b \sin 2\varphi}{a + b\cos\varphi}\right)\right] (r + b)^3} \quad (50)$$

and for the border stress in the fillet:

$$(\tau_\varphi)_{r=b} = \frac{2M}{\pi \cdot (a - b)^3} \cdot \frac{(a - b)^3 \cdot (a + b\cos\varphi) \left(\frac{3}{2}\cos\varphi + \frac{1}{4}\sin 2\varphi\right)}{(a - b\cos\varphi)^3 \left[a + b\cos\varphi \left(2 + \frac{b \sin 2\varphi}{a + b\cos\varphi}\right)\right]} = \frac{2M}{\pi \cdot (a - b)^3} \cdot \lambda_2 \quad (51),$$

where λ_2 represents the stress increase over the normal circumferential stress of the weaker part of the shaft. With $\varphi = 0$, eq. (51) transforms into eq. (47). As we can see, the maximum stress does not occur at the border point $\varphi = 0$, but at a closely neighboring border point $\varphi = \varphi_m$, and φ_m becomes maximum for $a/b = \infty$, i.e., for $b = 0$. Substituting $b = 0$ in eq. (51), the condition for maximum is:

$$\frac{d}{d\varphi} \cdot \left(\frac{3}{2}\cos\varphi + \frac{1}{4}\sin 2\varphi\right) = 0,$$

from which we get: $\sin\varphi_m = 0.281$ or $\varphi_m = 16°20'$. We thus find for $(\lambda_1)_{max}$:

$$(\lambda_1)_{max} = 1{,}57, \quad \text{WHILE} \quad (\lambda_1)_{\varphi=0} = 1{,}50$$

For the case of $a/b = 11$ we have $\varphi_m \cong 10°$ and the true maximum stress is only $3^1/_2\%$ larger than $(\tau_\varphi)_{\substack{r=b \\ \varphi=0}}$; for smaller values of a/b the difference is still less. The stress $(\tau_\varphi)_{\substack{r=b \\ \varphi=0}}$ of formula (47) can therefore be considered as the maximum stress with sufficient accuracy (see in this connection the last two columns of Table 11). The stress in the cross section $\varphi = 0$ obeys the law:

$$(\tau_z)_{\varphi=0} = \frac{2M}{\pi (a - b)^3} \cdot \frac{(a - b)^3 \cdot (z)^3_{\varphi=0} (a + b)(r^2 + 2rb + 3b^2)}{a^3 \cdot (a - r)^3 \cdot (a + 2b)(r + b)^3} = \frac{2M}{\pi \cdot (a - b)^3} \cdot \lambda_3 \quad (52),$$

and the radial stress component on the radius vector $\varphi = 0$ of the longitudinal section is

$$(\tau_r)_{\varphi=0} = \frac{2M}{\pi\cdot(a-b)^3}\cdot\frac{(a-b)^3\cdot(r)^3_{\varphi=0}\cdot 2b^2\cdot(r-b)}{a^2(a+2b)(r-b)^2\cdot r\cdot(r+b)}\left[\frac{r+2b}{a+2b}-\frac{a+b}{r+b}\right] = \frac{2M}{\pi\cdot(a-b)^3}\cdot\lambda_4 \quad (53).$$

The quantity in brackets is always negative, hence the two stress components on the radius vector $\varphi = 0$ always have opposite signs, as is also postulated by the pattern of the stress lines. The border stress of the stronger shaft part becomes:

$$(\tau_r)_{\varphi=\pi/2} = \frac{2M}{\pi\cdot a^3}\cdot\frac{(r-b)(r^2+3rb+4b^2)}{r(r+b)^2} = \frac{2M}{\pi\cdot a^3}\cdot\lambda_5 \quad . \quad . \quad . \quad . \quad (54).$$

The border stress of the weaker part of the shaft follows from the stress function F' which holds true for the region to the left of the radius vector $\varphi = 0$ (see Fig. 11) (when setting up this function we must remember that the angle φ here is negative and that the limiting condition on the border is $\overline{F}' = Ca^4$ for $r = \frac{b}{\cos\varphi}$). Thus, the equation for the above-mentioned border stress is

$$\tau' = \frac{1}{\cos\varphi}(\tau_\varphi)_{r=\frac{b}{\cos\varphi}} = \frac{2M}{\pi\cdot(a-b)^3}\frac{(a+b\cos\varphi)\left[1+\cos\varphi\left(2-\frac{\sin 2\varphi}{1+\cos\varphi}\right)\right]}{\left[a+b\cos\varphi\left(2-\frac{b\cdot\sin 2\varphi}{a+b\cos\varphi}\right)\right](1+\cos\varphi)} \quad . \quad .$$

$$= \frac{2M}{\pi\cdot(a-b)^3}\cdot\lambda_6 \quad . \quad . \quad . \quad . \quad . \quad . \quad . \quad . \quad . \quad . \quad . \quad . \quad . \quad . \quad . \quad . \quad . \quad . \quad . \quad (55).$$

This equation as well as eq. (54) were tested experimentally and good agreement was found (see test report). Fig. 12 shows the variation of the border stress along the border line of the meridional section of the shaft graphically, for the case: $a/b = 11$. The calculated stresses are plotted orthogonally to the contour line. Note the interesting phenomenon that the stress disturbance which is generated through the place of transition propagates much farther into the thin part of the shaft than into the thicker one. For instance, the deviation from the normal circumferencial stress that prevails on the thinner part of the shaft is about 8%, at an axial distance from the center of the fillet that equals six times the fillet radius. The deviation at the thicker part of the shaft, at an equal distance from the corner (at which the stress is zero) is on the other hand only one percent, in good agreement with the experimental results. Furthermore, it follows both from theory and experiment that the border stress of the stronger shaft part increases from the corner on faster than in the case of the grooved shaft.

Fig. 13 shows graphically the proportionality values $\frac{\tau_{max}}{\frac{2M}{\pi a^3}} = p_1$ and $\frac{\tau_{max}}{\frac{2M}{\pi\cdot(a-b)^3}} = p_2$ as functions of a/b, where τ_{max} is

the actual maximum stress at the border point $\omega = \omega_m$. The values found by Willers, of which only two were available here, are indicated by small circles. The agreement is very good here, too. For the case of a/b = 1, i.e., when the diameter of the thinner shaft becomes infinitesimally small, $\frac{\tau_{max}}{\frac{2M}{\pi a^3}}$ must become infinitely large and $\frac{\tau_{max}}{\frac{2M}{\pi \cdot (a-b)^3}}$ must become 1; $\frac{\tau_{max}}{\frac{2M}{\pi a^3}}$ will therefore approach the value ∞ asymptotically. For very large values of a/b both curves will approach the value 1.57 asymptotically.

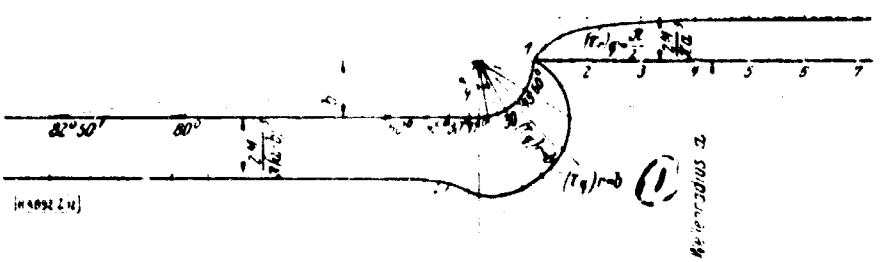

Fig. 12.

1 -- Shaft radius.

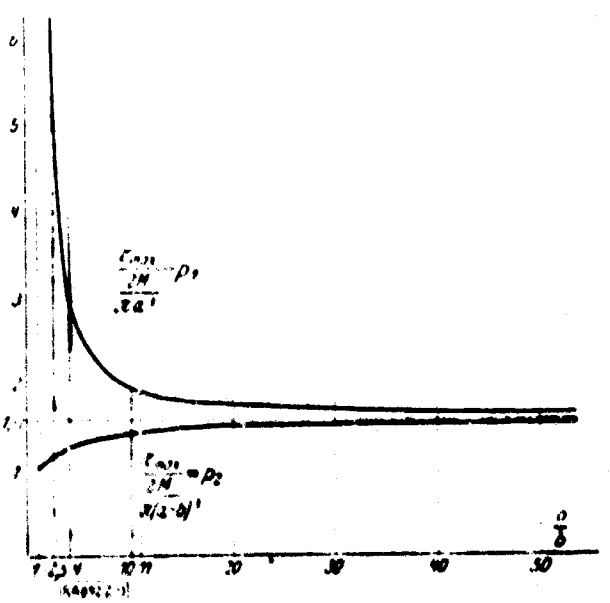

Fig. 13.

The behavior of the cross sectional stress $(\tau_\varphi)_{\varphi=0}$ eq. (52) and the radial component of the meridional sectional stress $(\tau_r)_{\varphi=0}$ eq. (53) along the radius vector $\varphi = 0$ is shown for a/b = 11 in Fig. 14. In Fig. 15 the tangents to the stress lines in the meridional section are plotted for different points of the radius vector $\varphi = 0$.

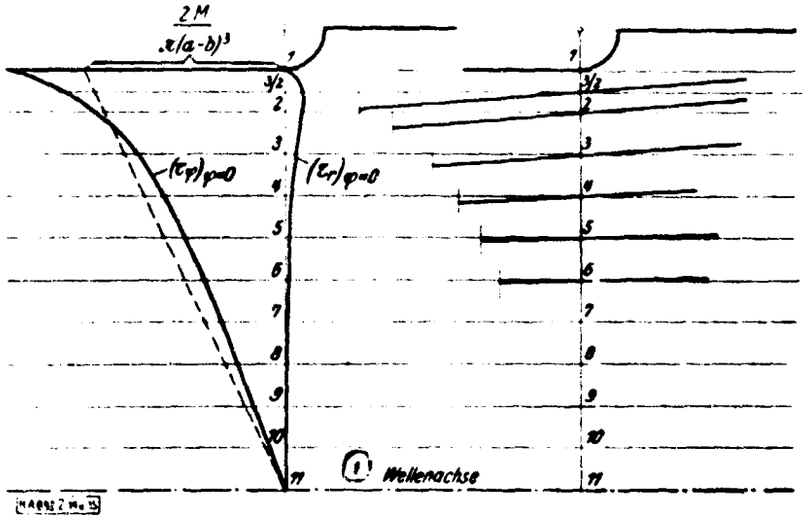

Figs. 14 and 15.

1 -- Shaft Axis.

The numerical values of the stresses have been computed for the drawing of the corresponding curves and are compiled in Tables 8 through 13.

TABLE 8.

$(\tau_\varphi)_{r=b} = \frac{2M}{\pi (b_0 - b)^3} \cdot \lambda_2$, (1) für den Fall: $\frac{a}{b} = 11$, (2) vergl. Abb. 12

φ	0°	10°	20°	30°	45°	60°	74°	90°
λ_2	1,385	1,43	1,424	1,35	1,23	0,922	0,55	0

1 -- For the case; 2 -- See Fig. 12.

6. Stepped Shaft, as in Fig. 11, but With Concentric Bore Hole. Using g to denote the radius of the bore, we obtain the following formula for the maximum stress, from a calculation that proceeds analogously to the previous case, which however we omit here

$$(\tau_\varphi)_{\substack{r=b \\ \varphi=0}} = \frac{2M \cdot a}{\pi \cdot (a^3 - g^3)\left[2(a^3 - b^3)(a - g + b) - \dots\right]} \cong \tau_{max.} \qquad (56)$$

TABLE 9.

$(v_r)_{\varphi=0} = 2\sqrt{\frac{2M}{\pi \cdot a^3}} \cdot \lambda_5$, für den Fall: $\frac{a}{b} = 11$, vergl. Abb. 12

$\frac{r}{b}$	1	1,2	1,5	1,7	2	3	4	6	10
λ_5	0	0,314	0,574	0,677	0,78	0,917	0,96	0,987	0,998

1 -- For the case; 2 -- See Fig. 12.

TABLE 10.

$v' = \sqrt{\frac{2M}{\pi \cdot (a-b)^3}} \cdot \lambda_6$, für den Fall: $\frac{a}{b} = 11$, vergl. Abb. 12

φ	0°	11°	30°	45°	60°	80°	82° 50'	85°	88°
λ	1,385	1,295	1,17	1,109	1,098	1,088	1,073	1,058	1,027

1 -- For the case; 2 -- See Fig. 12.

TABLE 11.

$(v_{\varphi=0})_{r=\infty} = v_{max} = \sqrt{\frac{2M}{\pi a^3}} \cdot p_1 = \sqrt{\frac{2M}{\pi \cdot (a-b)^3}} \cdot p_2$, vergl. Abb. 13

$\frac{a}{b}$	1	2,5	4	10	11	20	30	50	∞
p_1 (2)	∞	3,42	3,01	1,945	1,905	1,74	1,68	1,635	1,574
$(p_1)_\infty$ (nach Willers)	∞		2,95		1,905				
$\frac{p_1 - (p_1)_\infty}{(p_1)_\infty} \cdot 100$	0		+2		± 0				
p_2	1	1,17	1,27	1,42	1,43	1,49	1,52	1,54	1,574
λ_1	1	1,185	1,25	1,375	1,385	1,432	1,453	1,472	1,50

1 -- See Fig. 13; 2 -- (according to Willers).

TABLE 12.

$(v_\varphi)_{\varphi=0} = \sqrt{\frac{2M}{\pi (a-b)^3}} \cdot \lambda_8$, für den Fall $\frac{a}{b} = 11$, vergl Abb 14

$\frac{r}{b}$	1	1,5	2	3	4	5	7	9	11
λ_8	1,845	1,105	0,981	0,788	0,696	0,695	0,811	0,140	0

1 -- For the case; 2 -- See Fig. 14.

TABLE 13.

$(\sigma_r)_{\varphi=0} = \frac{2M}{\pi (a-b)^3} A_0$. (1) für den Fall: $\frac{a}{b} = 11$. (2) vergl. Abb. 14

$\frac{r}{b}$	1	1.5	2	3	4	5	7	9	11
A_0	0	− 0,084	− 0,079	− 0,048	0,027	− 0,015	− 0,04	0,0007	0

1 -- For the case; 2 -- See Fig. 14.

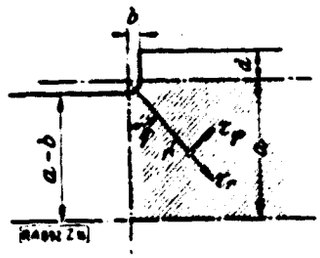

Fig. 16.

7. The Stepped Shaft Whose Step Height is Larger Than the Transition Radius (Fig. 16). For the sake of brevity we shall discuss here only the problem of the magnitude of the maximum stress. Here, too, this can be with sufficient accuracy by the stress at border point $\varphi = 0$. As we have pointed out already in Section 5, the term of the stress function containing φ with an odd exponent does not play any role, so, in order to calculate the stress we may neglect this term a priori. According to the procedure in Section 5 and with this simplification, we obtain for the stress function

$$F = K \left[a - r \cdot t_1 \left(\frac{b}{r} \right)^2 + t_2 \left(\frac{r+2b}{r-b} \cos\varphi \right)^4 = K \cdot a^4 \right. \qquad (57),$$

where

$$K = \frac{M}{\pi (a+d)^4}$$

In the following considerations we are concerned only with that region of the longitudinal shaft section that is cross hatched in Fig. 16. The same limiting conditions apply to it as to the case discussed in Section 4 and we find from this the coefficients t_1 and t_2 as

$$t_1 = \frac{2 \cdot \frac{d}{a} + \frac{a}{a+b\cos\varphi}}{2b \cdot \cos\varphi \cdot \frac{a+2b\cos\varphi}{a-b\cos\varphi}}, \qquad t_2 = \frac{2 \cdot \frac{d}{a} + \frac{a}{a+b\cos\varphi}}{3 \cdot \frac{a+2b\cos\varphi}{a-b\cos\varphi}} \qquad (58).$$

From eq. (57) we obtain:

$$(\sigma_r)_{\varphi=0} = \frac{2M}{\pi (a-b)^3} \frac{a-b}{a+d} \left[\frac{a}{b} - 2 - r \left(t_1 \frac{b}{r} + t_2 \frac{b}{r} \right) \right] \qquad (59)$$

and

$$(\sigma_\vartheta)_{\varphi=0,\, r=b} = \sigma_{max} = \frac{2M}{\pi (a-b)^3} \frac{a-b}{a+d} \left[\frac{1}{3} t_2 - \frac{1}{6} t_1 \right]$$

$$\frac{2M}{\pi (a-b)^3} \frac{1}{2(a+d)} \left[\frac{2a \cdot a + b}{a+2b} + \frac{d}{3} \left(3 + \frac{a}{b} \right) \right] = \frac{2M}{\pi (a-b)^3} A \qquad (60)$$

For $d = 0$ we get $\mu = \frac{3}{2} \cdot \frac{a + b}{a + 2b}$, as is also postulated by the analogy to the case of Section 5.

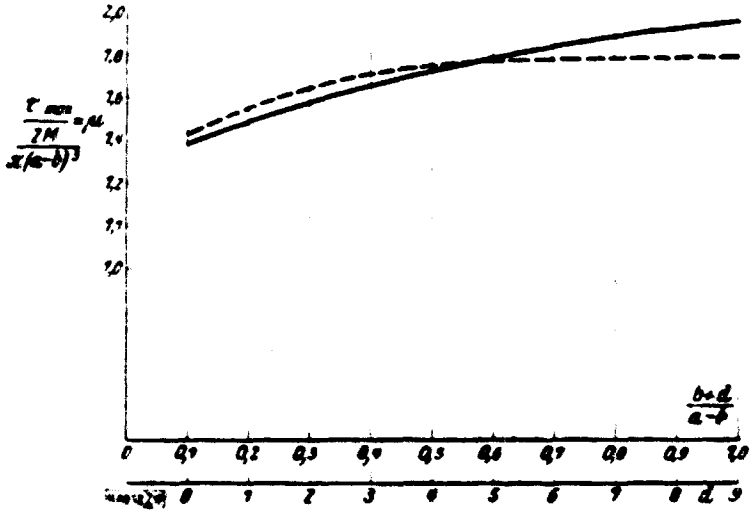

Fig. 17.

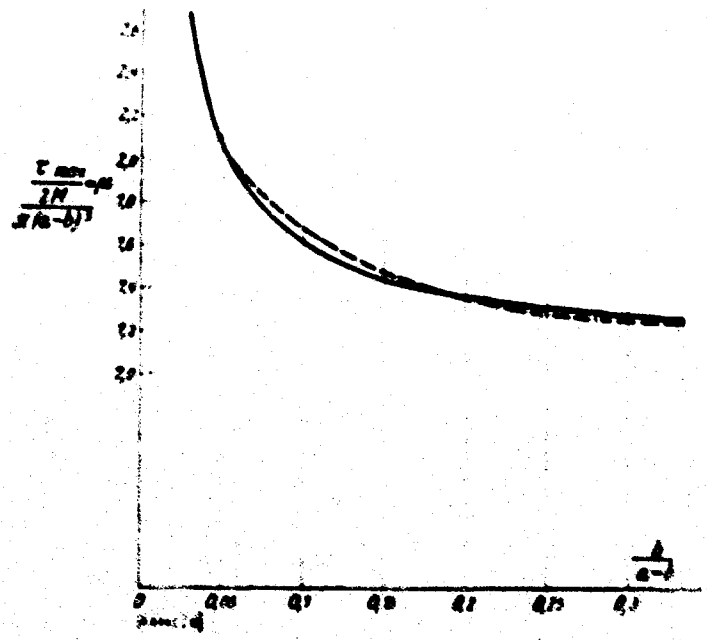

Fig. 18.

For $b = 0$, i.e., on a sharp corner, $\mu = \infty$. Fig. 17 shows the factor μ, which characterizes the stress increase, as a function of $\frac{b + d}{a - b}$ for the case of $a/b = 11$. This curve is drawn as a solid line. The curve obtained by Willers is drawn as a dashed line (see also Table 14). When we compare these two curves and also the following ones, we must take into

account that the Willers values refer to the actual maximum stresses, whereas we have approximated them in this problem by the border stresses $(\tau_{r\varphi})_{\substack{r=b \\ \varphi=0}}$ which are slightly smaller. For instance (see also Table 14) the following appears: The factor μ is 1.385 for $\frac{b + d}{a - b} = 0.1$, i.e., for $d = 0$, while the maximum stress increase as calculated in Section 5, for the border point $\varphi = \varphi_m$ yielded for this case the value 1.43, which agrees with Willers. Taking this into consideration we can say that the two curves exhibit satisfactory agreement. Only at relatively large values of d/a are the deviations greater, but these cases are no longer of any practical significance. The solid-line curve in Fig. 18 shows the factor μ as a function of $\frac{b}{a - b}$ for the case $\frac{a - b}{a + d} = \frac{3}{4}$ (see also Table 15). Here too, the computed values agree beautifully with those of Willers (dashed curve). It can be seen from these two curves that the increase in the ratio of the shaft radii $\frac{a + d}{a - b}$ at constant fillet radius causes an increase in the maximum stress (Fig. 17), while, when the ratio of the shaft radii is kept constant but the ratio of the fillet radius to the smaller shaft radius is increased, the maximum stress decreases (Fig. 18). Willers varied these two ratios of the radii simultaneously, in the same sense, by taking the shaft contour as an unchanging entity and putting it closer to or farther away from the axis, whereby it was to be expected that the stress increase remains nearly constant. The same experiment has been made here, in Fig. 19, for the case that $b = 1/2(d + b)$, i.e., that the fillet radius comprises one third of the shaft step. Fig. 19 shows the variation of the stress increase at increasing distance of the shaft contour from the axis; the dashed curve is again taken from the paper by Willers[1] (see also Table 16). As can be seen from the calculated curve, the constancy of factor μ is out of the question, if only for the reason that the curve has to intersect the ordinate axis at point 1 in any case. This is explained from the fact that there can be no stress increase for a shaft for which $a - b = 0$, i.e., a shaft whose fillet radius is infinitely large as compared with the radius of the thinner shaft part. It seems that μ approaches a constant value only at higher values of a - b. This proves that our approximation theory permits the calculation of the

1) Dr Willers told me in answer to an inquiry that the ordinates of this curve (Fig. 13 of Willers' dissertation) belonging to the values of a - b, especially to the small values, are erroneously given as far too large. So, for instance, according to Willers, the stress increase for a - b = = 3 is not 61%, as stated in the dissertation referred to, but only 2%.

strength of also those shafts which are most important in practice with an accuracy which is absolutely sufficient for technical applications -- with the single exception of exaggerated sharp and abrupt diameter changes which in any case must always be avoided in practice. For this kind of shafts our calculation yields values of the stress increase which are slightly too high[1].

TABLE 14.

$(\tau_\varphi)_{\substack{r=b \\ \varphi=0}} \sim \tau_{max} = \frac{2M}{\pi \cdot (a-b)^3 \cdot \mu}$, für den Fall: (1) $\frac{a}{b} = 11$, vergl. hierzu (2) Abb. 17

$\frac{b+d}{a-b}$	0,1	0,2	0,3	0,5	1,0	∞
$\mu(\varphi=0)$ (3)	1,385	1,49	1,581	1,726	1,96	2,66
$\mu_w(\frac{\tau}{\tau_m})$ (nach Willers)	1,43	1,55	1,62	1,75	1,79	—
$\frac{\mu-\mu_w}{\mu_w} \cdot 100$	− 3,1	− 3,9	− 4,2	− 1,4	+ 9,5	--

1 -- For the case; 2 -- See also Fig. 17; 3 -- (according to Willers).

TABLE 15.

$(\tau_\varphi)_{\substack{r=b \\ \varphi=0}} \sim \tau_{max} = \frac{2M}{\pi (a-b)^3 \cdot \mu}$, für den Fall: (1) $\frac{a-b}{a+d} = \frac{3}{4}$, vergl. hierzu (2) Abb. 18

$\frac{b}{a-b}$	0	0,05	0,1	0,2	0,25	0,33
$\mu(\varphi=0)$ (3)	∞	2,05	1,61	1,36	1,31	1,25
$\mu_w(\frac{\tau}{\tau_m})$ (nach Willers)	∞	2,05	1,675	1,35	1,275	1,24
$\frac{\mu-\mu_w}{\mu_w} \cdot 100$	±0	±0	− 3,9	+ 0,7	+ 2,7	+ 0,8

1 -- For the case; 2 -- See also Fig. 18; 3 -- (according to Willers).

1) For instance, according to our calculation the stress at a sharp corner approaches infinity as $\lim_{b=0} \frac{c}{b}$, whereas, as Willers has shown, it becomes infinite as $\lim_{b=0} \frac{c}{\sqrt[3]{b}}$.

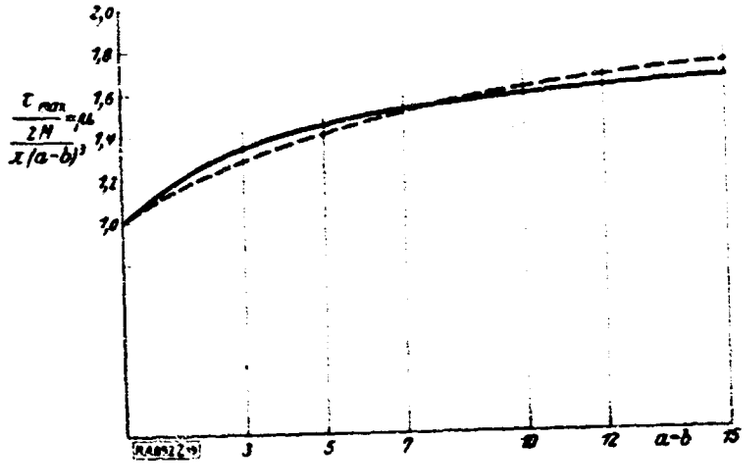

Fig. 19.

TABLE 16.

$\tau_{z\varphi}\big\|_{z=0} = \tau_{max} = \frac{2M}{\pi (a-b)^3} \cdot \mu$, für den Fall: $b = \frac{1}{3}(d+b) = 1$, vergl. hierzu Abb 19						
$a-b$	3	5	7	10	12	15
$\mu(z=0)$ (3)	1,333	1,44	1,51	1,58	1,606	1,65
$\mu(z=\tau_{max})$ (nach Willers)	1,28	ca. 1,40	ca. 1,50	ca. 1,60		ca. 1,72
$\frac{\mu - \mu_w}{\mu_w} \cdot 100$	+ ca. 4	+ ca. 3	ca. 0	ca. 0		ca. 4

1 -- For the case; 2 -- See also Fig. 19; 3 -- (according to Willers).

8. Danger of Fracture at Abrupt Transition. In this connection we shall make a few short remarks on the danger to which such a stepped or grooved shaft with relatively very small fillet radius is exposed. As has been shown (see e.g., Fig. 9) the region in which the stress increase is noticeable when compared with linear distribution is locally confined within narrow limits. Let us suppose that the shaft was designed and dimensioned for a certain load without regard to the stress increase at the transition point. If, now, this load is applied only once, the calculated maximum stress will not be formed in the fillet in the case of a plastic material, because after the elasticity limit has been exceeded at the place of highest stress and the plastic flow of the material begins, a plastic state of stress sets in over a very small region which is entirely different from the calculated elastic state. In such a case even a very large calculated stress increase would normally hardly endanger the shaft seriously. But in contrast to a non-recurrent, single loading, a varying load is of uncomparably higher importance: it will inexorably bring such a

shaft as described above in course of time to a fatigue breakdown, because the over stresses, repeated innumerable times, form crystalline planing surfaces and cause at last fine hair cracks[1]. So, for instance, all shafts having abruptly changing diameters and being subjected in operation to oscillations (e.g., tunnel and propeller shafts of ship engines[2], shafts of steam turbines, crank shafts of Diesel engines, etc.) belong to the machine parts carrying highest strains, and an exact knowledge and consideration of their stress increases on the transition points is of great, and sometimes crucial importance[3].

9. The Experiments which have been performed in the Strength of Materials Laboratory of the Polytechnical Institute of Munich[4] could have as their aim only the determination of the cylindrical part of the shafts that adjoin directly the place of transition, because it seems hardly possible to measure the stresses directly on the fillets. A semicircular groove was turned into the stronger part of the test shaft, according to Fig. 2, and the shaft was turned down to a smaller diameter at a sufficiently great distance from the groove and from the shaft ends. The transition was formed by a 90° circular arc according to Fig. 11. The shaft was made of S. M. steel of 7000 kg/cm^2 tensile strength and was cleanly ground on the cylinder parts. The pertinent dimensions were as follows: radius of the stronger part of the shaft: a = 4.4 cm, groove radius b_r = 0.4 cm, radius of the fillet on the step b_s = 0.41 cm. Thus, the ratio a/b for the groove is 11 and for the step: 10.7. The total free length of the shaft between the chucks was 140 cm. The experiments were performed on the large Werder-Machine which has a cross head for the attachment of the chucks for torsion experiments. The machine was freshly calibrated before the experiments.

---

1) See Th. v. Kármán and L. Föppl, Encyclopedia of Mathematical Sciences IV, 31, page 732.
2) See also e.g., K. Kutzbach: Common Problems in Machine Design, VDI-Zeitschr. 1915, page 849. A. Thum. Materials in Modern Steam Turbines, VDL-Zeitschr., 1927, page 754 and following.
3) See to this section especially: F. László: "The Notch," VDI-Zeitschr., 1928, page 851 and following.
4) I am very much indebted to the Head of the Laboratory, Prof. Dr. Föppl, for having placed necessary equipment and help at my disposal.

For the precision measurements we used the shear stress meter[1] designed by Dr.-Ing. K. Huber in München, which permits a very accurate measurement of the angular changes and hence of the stresses (if the shear modulus is given). The angular displacement of the two mirrors of the shearing meter was observed in the usual manner by telescope and graduated scale. The two points of the lever which rest on the generatrix of the shaft cylinder, when the instrument is attached, have a distance from each other of 10 mm. Hence, the measurement yields the mean value of the angular change (or of the shear stress) along a distance of 10 mm length. Instead of one reading dial two must be used, because otherwise the simultaneously occurring rotation in a perpendicular plane, which the shearing meter experiences together with the shaft, moves the image out of the field of view of the telescope and thus renders a reading impossible. The just-mentioned rotation of the mirrors also had for consequence that we operate only with a relatively light loading because otherwise the two dials would have to be too far apart, which would have impaired the accuracy of the reading. The distance of the dial from the axes of the two mirrors, i.e., from the center of the shaft, was 1500 mm, so that when the dial readings of the two mirrors are a_1 and a_2 in mm, the angular change γ was: $\gamma = \frac{a_1 + a_2}{63000}$, provided that the two mirrors rotate in opposite directions -- which was the case in the experiments.

The following relation exists between the shear stress τ, the angular displacement γ and the shear modulus G: $\tau = \gamma \cdot G$. Therefore, the shear modulus of the shaft material was first determined. This was done in the following way: the angular change γ was measured on both the stronger and weaker parts of the shaft, at a sufficient distance from the shaft ends and the transition points and then τ was calculated from the well known formula $\tau = \frac{2M}{\pi \cdot a^3}$. The lever arm of the torsional moment was 49.6 cm, the load range which was found most suitable and hence used in almost all experiments, was 750 - 500 = 250 kg, so that the torsional moment was M = 250 · 49.6 = 12400 kg/cm [sic. should read kg cm]. The following mean values from five experiments resulted from the weaker part of the shaft:

---

1) K. Huber, VDI-Zeitschr., 1923, page 923, "The Determination of the Shear Stresses and the Elasticity Modulus of Shearing by Means of a New Precision Instrument." A. Föppl gives a detailed description of the shear stress meter in the Reports of the Meetings of the Bavarian Academy of Sciences, 1923, page 109.

$$a_1 = 6{,}38 \text{ mm}, \qquad a_2 = 3{,}05 \text{ mm}, \qquad a_1 + a_2 = 9{,}43 \text{ mm}$$

and thus

$$\gamma = \frac{9{,}43}{63\,000}, \qquad \tau = \frac{2 \cdot 124\,000}{\pi \cdot 3.989^3} = 124{,}5 \text{ kg/cm}^2,$$

so that

$$G = \tau/\gamma = 834\,000 \text{ kg/cm}^2.$$

For the stronger shaft part, the mean value from seven experiments yielded

$$a_1 = 4{,}9 \text{ mm}, \qquad a_2 = 2{,}1 \text{ mm}, \qquad a_1 + a_2 = 7{,}0 \text{ mm}$$

thus

$$\gamma = \frac{7{,}0}{63\,000}, \qquad \tau = \frac{2 \cdot 124\,000}{\pi \cdot 4{,}4^3} = 92{,}7 \text{ kg/cm}^2,$$

from which

$$G = \tau/\gamma = 834\,000 \text{ kg/cm}^2.$$

The complete agreement of these two values for G proves that the precision instrument is very reliable.

Accordingly, 1 mm of the dial graduation means a shear stress of $\tau = \frac{834{,}000}{63{,}000} = 13.23$ kg/cm^2 and since 1/10 mm can well be estimated during the reading, the mean value of the shear stress along a measuring distance of 10 mm can be determined to an accuracy of 1 to 1.5 kg/cm^2 if one succeeds in eliminating all other experimental errors.

The additional frictional moment on the movable chuck by which the torsional moment is transmitted to the shaft was practically without any influence upon the experiments because the angular displacements were measured not starting at the zero load but within the load range of 500 to 750 kg. (In a few cases, the load range 750 to 1000 kg was also used as far as possible.) Only those experiments were considered admissible for the computation of the mean value for which the readings before loading and after unloading agreed completely or differed only by a few tenths. If after unloading the zero reading on the left telescope was greater by the same amount (compared with the zero reading before loading) as the reading was lower on the right telescope, this showed only that the shaft had moved during the experiment. Such an experiment was therefore still considered all right.

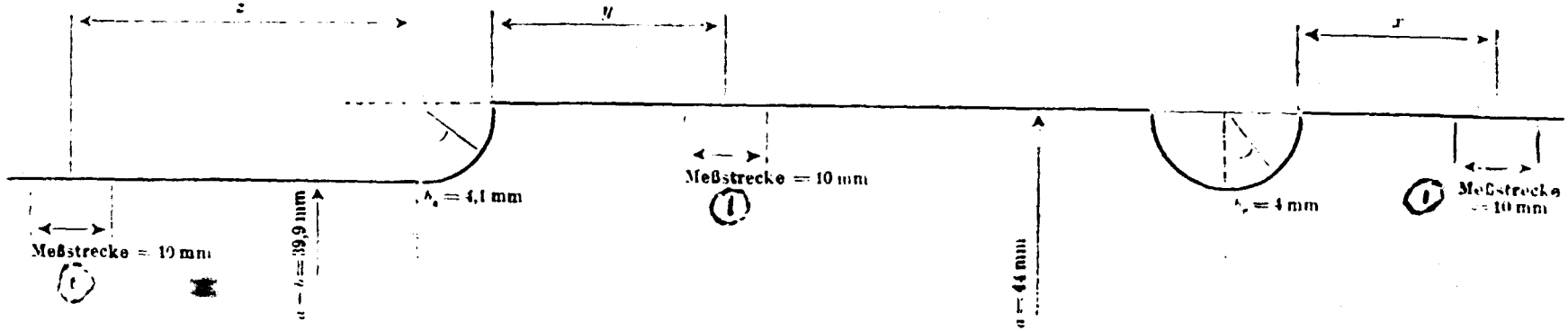

(2) Meßstelle	(3) Drehmoment M in cm/kg	(4) Mittelwert der Skalenablesungen aus durchschnittlich je vier Versuchen $a_1 + a_2$ in mm	(5) Mittelwert der Schubspannung τ innerhalb d. Meßstrecke von 10 mm (6) a) Versuch $\tau_e = (a_1 + a_2) \cdot \frac{834}{63}$ in kg/cm²	(7) b) Rechnung τ_r in kg/cm²	$\frac{\tau_r - \tau_e}{\tau_r} \cdot 100$
$x = 6{,}2$ mm	124 000	5,8	76,8	74	+ 3,6
$x = 11{,}5$ »	»	6,5	86,0	85,7	+ 0,3
$x = 15$ »	»	6,7	88,6	88,2	+ 0,5
$x = y = 200$ »	»	7,0	92,7	92,7	± 0
$y = 5{,}5$ »	»	5,65	74,8	72,8	+ 2,7
$y = 9$ »	»	6,55	86,7	84,5	+ 2,4
$y = 13$ »	»	6,7	88,6	88,4	+ 0,2
$z = 5{,}2$ »	»	10,27	136	141	− 3,6
$z = 25$ »	»	10,03	133	135	− 1,5
$z = 250$	»	9,43	124,5	124,5	± 0

1 -- Measuring Distance; 2 -- Location of measurement; 3 -- Torsional Moment in cm/kg [sic. should read cm kg.]; 4 -- Mean value of dial readings from four experiments on the average; 5 -- Mean value of the shear stress τ within the measuring distance of 10 mm; 6 -- a) Experiment; 7 -- b) Calculation.

Page 35 of the manuscript shows the test report for the stress measurements at the different locations on the shaft. The agreement in the shear stresses found by computation and by experiment may be considered satisfactory if we remember that the calculation is an approximation only and that the experiments were performed, for the reason stated above, at a relatively very small load range in which reading errors and other experimental errors play a larger role than in the case with a larger load range.

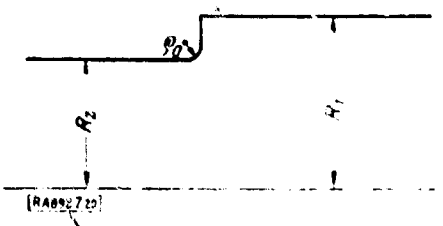

Fig. 20.

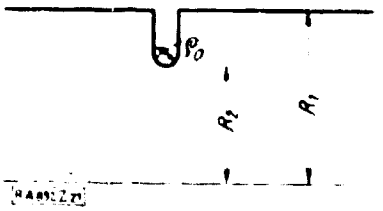

Fig. 21.

Summary. A simple approximation method is shown for the calculation of stress increases at the transition points of stepped or grooved shafts. The results of this method are well confirmed by the paper of Willers as well as by our own experiments. This method depicts the actual conditions for practically all technically important cases with a completely sufficient accuracy. (The average error is less than ±5%.) Somewhat larger deviations -- meaning higher computed maximum stresses -- will probably result for exceptionally abrupt transitions, i.e., in cases which are obviously dangerous and are therefore in practice of minor interest only, apart from the fact that they can always be avoided. With the notations of Figs. 20 and 21, which are commonly used in practice, the formulae for the maximum stresses are:

1. For a stepped shaft according to Fig. 20:

$$\tau_{max} = \frac{2M}{\pi \cdot R_2^3} \cdot \frac{1}{2R_1}\left[\frac{3(R_2+\rho_0)(R_2+2\rho_0)}{R_2+3\rho_0} + \frac{(R_1-R_2-\rho_0)(R_2+6\rho_0)}{3\rho_0}\right].$$

In the frequent case: $R_1 - R_2 = \rho_0$, this formula simplifies to

$$\tau_{max} = \frac{2M}{\pi \cdot R_2^3} \cdot \frac{3(R_1+\rho_0)}{2(R_1+2\rho_0)}.$$

2. For a shaft with a turned-in groove according to Fig. 21:

$$\tau_{max} = \frac{2M}{\pi \cdot R_2^4} \cdot \frac{(R_2+\rho_0)^3 (R_1-R_2) + (R_2+\rho_0)^2 \rho_0 (R_1-R_2-\rho_0)}{\rho_0 \, R_1 (R_2+2\rho_0)}.$$

For a shaft with semicircular groove ($R_1 - R_2 = \rho_0$) we have

$$\tau_{max} = \frac{2M}{\pi \cdot R_2^3} \cdot \frac{r_1}{R_1 + \rho_0}.$$